Sensors and Actuators B 204 (2014) 50–56

Contents lists available at ScienceDirect

Sensors and Actuators B: Chemical

journal homepage: www.elsevier.com/locate/snb

Dynamics and response of a humidity sensor based on a Love wave device incorporating a polymeric layer

Jiansheng Liu*, Lijun Wang

Institute of Acoustics, Chinese Academy of Sciences, Beijing 100190, China

ARTICLE INFO

Article history:
Received 6 May 2014
Received in revised form 11 July 2014
Accepted 22 July 2014
Available online 30 July 2014

Keywords:
Surface acoustic wave
Love wave
Humidity
Viscoelastic
Adsorption

ABSTRACT

In this study, we investigate the dynamics and response of a humidity sensor based on a polymer-coated Love wave device. A review is presented for the theoretical model of Love waves in a layered structure with a viscoelastic layer on a piezoelectric substrate. Numerical illustrations are executed for the mass velocity sensitivity and mass loss sensitivity of a polymer-coated device. The BET equation and its improved equation are introduced to describe the adsorption mechanism of gas on the detector surface. A method is introduced for calculating the surface area of the polymer layer, which is proved a porous material. An experiment is performed for a humidity sensor based on a Love wave device consisting of two 28 μm-periodic interdigital transducers, a 0.47 μm-thick PVA layer, and an ST-90°X quartz substrate. The operation frequency and insertion loss of the Love wave device are measured by using a network analyzer; the relative surface area of the PVA layer is calculated through comparing the fitted and the theoretical frequency shift caused by the monolayer of water molecules. The frequency shifts and insertion loss increments are shown as functions respect to the relative humidity; the theoretical curves agree well the experimental results.

© 2014 Elsevier B.V. All rights reserved.

1. Introduction

In the past few decades, surface acoustic wave (SAW) sensors [1–3] have been attracting the interest of many researchers because of their high sensitivity, small size, low cost, and easy fabrication. SAWs are excited and received by the interdigital transducers (IDTs) deposited on the surface of a piezoelectric substrate. Due to the surface energy concentration, SAWs are very sensitive to the disturbance acting on the substrate surface. Using this feature, SAWs have broad prospects in many sensing areas such as temperature [4], pressure [5], strain [6], acceleration [7], mass loading, etc. Wherein SAW gas sensors [8,9], a type of sensor for mass loading, are often coated with sensing films to achieve higher sensitivities and the selective adsorption of a target gas. Because of their simple coating and good selectivity, polymers are often used as sensitive films for SAW gas sensors.

Humidity is of great importance in varieties of commercial and industrial applications, so humidity sensors have been attracting the interest of many researchers [10]. For a humidity sensor based on SAW technology, one of the most important design considerations is the choice of sensitive film. The most common sensitive films are polymers [11–14] with strong hygroscopicity, which is helpful to obtain a larger output response. However, the insertion loss of the detector will also increase due to the polymer's viscoelasticity.

Love wave is a kind of SAW which propagates in a layered structure. The substrate of a Love wave device supports a purely (or predominantly) piezoelectric shear horizontal (SH) acoustic wave which is faster than the transverse wave in the upper layer. Because of the particle polarization only existing in the SH direction, almost no energy is coupled into the liquid above the layer, thus Love waves are also suitable for detection in liquids. Different from a commonly used Rayleigh type SAW device, the performance of a Love wave device depends on its guiding layer rather than on IDT structures and substrate characteristics. A suitable guiding layer is the key to implement a Love wave sensor with high mass sensitivity, good temperature stability, and acceptable insertion loss. Due to its low acoustic loss and excellent abrasion resistance, SiO_2 is the most used guiding layer material for Love wave devices. Unfortunately, a Love wave sensor incorporating a SiO_2 layer cannot achieve a very high sensitivity, because of the fast transverse acoustic waves in SiO_2. Due to their low shear waves, polymers are often adopted as guiding layers for Love wave sensors to get a higher sensitivity.

The shortcoming of polymeric layer is the large loss caused by the viscosity of polymers. To analyze the effect of the viscosity, many theoretical models have been developed for SAW devices

* Corresponding author. Tel.: +86 1082547803.
E-mail addresses: liujs98@hotmail.com, liujiansheng@mail.ioa.ac.cn (J. Liu).

http://dx.doi.org/10.1016/j.snb.2014.07.095
0925-4005/© 2014 Elsevier B.V. All rights reserved.

incorporating polymeric layers. Based on perturbation approach, Martin et al. [15] investigated the dynamics and response of polymer-coated SAW devices with acoustically thin and thick layers. They committed that the changes in velocity and attenuation caused by the viscoelastic film were related to the surface mechanical impedances contributed by the film. By expanding the complex dispersion equation into Taylor series, Kielczynski [16] analyzed Love wave devices incorporating a low loss guiding layer. By adopting Maxwell model to describe the viscoelasticity of polymer layers, McHale et al. [17] developed a method for describing Love wave sensors incorporating viscoelastic guiding layers. In our previous works [18,19], the authors reported a method for Love wave devices consisting of a polymeric layer on a piezoelectric substrate by adopting a Maxwell–Weichert model to describe the viscoelasticity of the guiding layer.

For gas sensors, another key element is the adsorption mechanism of gas on detector surface, which describes the relationship between the adsorption amount and the gas concentration. In past decades, many experimental studies [11,20–22] were carried out to measure the curves of SAW velocity (or oscillation frequency) changes versus different gas concentrations. However, theoretical research was rarely reported on the gas adsorption mechanism in the field of SAW sensors. In our recent paper [23], the gas adsorption mechanism was described by adopting a Brunauer–Emmett–Teller (BET) equation and its improved form. Combined the Wohljent's theory, a theoretical method was developed for the response mechanism of SAW gas sensors based on surface adsorption. By using a commercial SAW gas chromatography (GC) analyzer, the method was verified by an experimental measurement of the frequency shifts caused by different concentrations of dimethyl methylphosphonate (DMMP).

In this study, we investigate the dynamics and response of a humidity sensor based on a polymer-coated Love wave device. Firstly a theoretical model is reviewed for Love wave device consisting of a polymeric layer and a piezoelectric substrate. The mass velocity sensitivity and the mass loss sensitivity are introduced for polymer-coated devices. Numerical illustrations are presented for a Love wave device with a polymeric layer on an ST-90°X quartz substrate. Secondly the BET adsorption equation is introduced to describe the physical adsorption of gas on solid surfaces. Anderson equation, a improved form of BET equation, is presented to expand the suitable scale of the adsorption equation. A method is introduced for calculating the surface area of the polymer layer. The response of SAW devices caused by gas adsorption is analyzed. In the experiment section, a humidity sensor is implemented based on a Love wave device consisting of a polyvinyl alcohol (PVA) layer on an ST-90°X quartz substrate. The response curves are measured for changes in operation frequency and insertion loss as functions respect to relative humidity (RH). Theoretical curves are also predicated by the developed method and they agree well with the experiment results.

2. Theoretical analysis on Love wave sensors

2.1. Dispersion equation and mass sensitivity

In this section, a review is presented on Love waves in a piezoelectric layered structure [24,25]. Fig. 1 displays the schematic of a Love wave device and the coordinate system used in this work. The propagation direction is parallel to the x_1-axis; the particle displacement is parallel to the x_2-axis, which is in the SH direction. The piezoelectric substrate occupies the lower half space of $x_3 < 0$; the non-piezoelectric layer occupies the internal space of $0 < x_3 < h$; the upper half space of $x_3 > h$ is occupied by the air which is assumed none mechanical touch on the layer surface. Material constants of

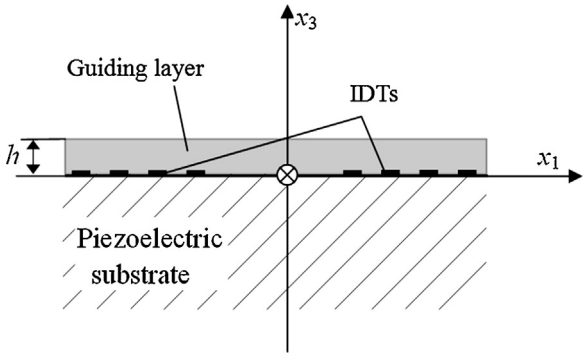

Fig. 1. Schematic and the coordinate system of a Love device.

the piezoelectric substrate must be in some special forms [26] to support pure SH acoustic waves coupled with electric fields.

In the piezoelectric substrate, the particle motion is coupled with the electric field, thus the particle displacement and the electric potential must satisfy the following equations:

$$c_{jk2l}\frac{\partial^2 u_2}{\partial x_k \partial x_l} + e_{k2l}\frac{\partial^2 \varphi}{\partial x_k \partial x_l} = \rho\frac{\partial^2 u_2}{\partial t^2}, \quad j = 1, 2, 3; \quad k, l = 1, 3 \tag{1}$$

$$e_{k2l}\frac{\partial^2 u_2}{\partial x_k \partial x_l} - \varepsilon_{kl}\frac{\partial^2 \varphi}{\partial x_k \partial x_l} = 0, \quad k, l = 1, 3 \tag{2}$$

where c, e, and ε are elastic, piezoelectric, and dielectric constants of the substrate respectively, ρ is the mass density, u_2 is the particle displacement in the x_2 direction, φ is the electric potential. Solutions of the shear acoustic wave and electric field in the substrate are:

$$u_2 = [M_1 A_1 \exp(k\beta_1 x_3) + M_2 A_2 \exp(k\beta_2 x_3)] \exp\{i(\omega t - kx_1)\} \tag{3}$$

$$\varphi = [M_1 \exp(k\beta_1 x_3) + M_2 \exp(k\beta_2 x_3)] \exp\{i(\omega t - kx_1)\} \tag{4}$$

where ω is the angular frequency, k is the wave number, β is the amplitude decaying factor in the $-x_3$ direction, M is the undetermined coefficient to be decided by the boundary conditions.

In the isotropic layer, the SH acoustic wave is uncoupled with the electric field and their solutions are in following forms:

$$u_2^L = [M_3 \exp(ik\beta_L x_3) + M_4 \exp(-ik\beta_L x_3)] \exp\{i(\omega t - kx_1)\} \tag{5}$$

$$\varphi^L = [M_5 \exp(kx_3) + M_6 \exp(-kx_3)] \exp\{i(\omega t - kx_1)\} \tag{6}$$

where $\beta_L = \sqrt{v^2/V_L^2 - 1}$, v is the propagation velocity of Love waves, $V_L = \sqrt{\mu_L/\rho_L}$ is the velocity of the transverse acoustic wave in the layer, and μ_L and ρ_L are the shear modulus and mass density of the layer medium respectively.

In the space above the layer, only the electric field exists and it can be described as:

$$\varphi^0 = M_7 \exp\{-k(x_3 - h)\} \exp\{i(\omega t - kx_1)\}. \tag{7}$$

The acoustic waves and electric fields must obey the following boundary and continuity conditions:

(1) At the interface of $x_3 = 0$, the continuity conditions for particle displacement, electric potential, normal stress and normal electric displacement for the electrically open case are:

$$\begin{cases} u_2(x_3 = 0) = u_2^L(x_3 = 0) \\ T_{23}(x_3 = 0) = T_{23}^L(x_3 = 0) \\ \varphi(x_3 = 0) = \varphi^L(x_3 = 0) \\ D_3(x_3 = 0) = D_3^L(x_3 = 0) \end{cases} \tag{8}$$

where T_{23} and T_{23}^L are the normal stresses in the substrate and the layer respectively, D_3 and D_3^L are the normal electrically displacements in the substrate and the layer respectively.

(2) At the layer surface of $x_3 = h$, the normal stress and the electrical conditions are:

$$\begin{cases} T_{23}^L(x_3 = h) = 0 \\ \varphi^L(x_3 = h) = \varphi^0(x_3 = h) \\ D_3^L(x_3 = h) = D_3^0(x_3 = h) \end{cases} \tag{9}$$

Substituting Eqs. (3)–(7) into the boundary and continuity conditions, and eliminating the undetermined coefficients M, we can get the dispersion equation of Love waves in a piezoelectric layered structure:

$$\mu_L \beta_L \tan(k\beta_L h) = \frac{(D_2 - \bar{\varepsilon}_L)T_1 - (D_1 - \bar{\varepsilon}_L)T_2}{(D_2 - \bar{\varepsilon}_L)A_1 - (D_1 - \bar{\varepsilon}_L)A_2} \tag{10}$$

where D and T are normal displacement and normal stress at the interface of $x_3 = 0$, $\bar{\varepsilon}_L$ is the equivalent permittivity of the guiding layer.

If the surface of the layer is covered by a mass load with an areal density of σ, the dispersion equation becomes:

$$\mu_L \beta_L \frac{\mu_L \beta_L \tan(k\beta_L h) + k\sigma v^2}{\mu_L \beta_L - k\sigma v^2 \tan(k\beta_L h)} = \frac{(D_2 - \bar{\varepsilon}_2)T_1 - (D_1 - \bar{\varepsilon}_2)T_2}{(D_2 - \bar{\varepsilon}_2)A_1 - (D_1 - \bar{\varepsilon}_2)A_2}. \tag{11}$$

The mass load will produce a perturbation in the propagation velocity of Δv, thus the mass sensitivity can be defined as:

$$S_m^v = \frac{1}{v}\frac{\Delta v}{\sigma} = \frac{2\pi}{\lambda}\frac{1}{v}\frac{\Delta v}{k\sigma}. \tag{12}$$

2.2. Love wave device incorporating a viscoelastic layer

In a linear system, the modulus of a viscoelastic material is often represented by a model consisting of springs and dashpots. In a Maxwell–Weichert model (also called generalized Maxwell model), the shear modulus of the polymeric layer can be considered as many branches connected in parallel. As presented in our previous work [18], the model can be simplified as an elastic branch and a Maxwell branch: the elastic branch consists of a spring, the Maxwell branch consists of a spring and a dashpot in serial. The complex shear modulus of the viscoelastic guiding layer can be described as:

$$\mu = \mu_0 + \mu_1 \frac{i\omega\tau_1}{1 + i\omega\tau_1} \tag{13}$$

where μ_0 corresponds to the modulus represented by the spring in the elastic branch, μ_1 corresponds to the modulus represented by the spring in the Maxwell branch, $\tau_1 = \eta_1/\mu_1$ is the relaxation time, η_1 corresponds to the viscosity represented by the dashpot. For the Love wave device incorporating a viscoelastic guiding layer, the propagation velocity becomes complex $v = v_r + iv_i$, and the propagation loss per wavelength can be described as:

$$\mathrm{IL} = 54.6\frac{s_i}{s_r} \approx -54.6\frac{v_i}{v_r} \tag{14}$$

where $s = 1/v$ is the slowness of Love waves.

The mass sensitivity obtained in Eq. (12) also becomes complex: $S_m^v = S_m^{v_r} + iS_m^{v_i}$, where $S_m^{v_r}$ is the mass velocity sensitivity for Love wave sensor incorporating a viscoelastic layer:

$$S_m^{v_r} = \frac{\Delta v_r}{v_r \sigma} = \mathrm{Re}(S_m^v). \tag{15}$$

$S_m^{v_i}$ indicates the attenuation caused by the mass load. The mass loss sensitivity of a polymer-coated Love wave sensor is:

$$S_m^{\mathrm{IL}} = -54.6\frac{\Delta v_i}{v_r \sigma} = -54.6\,\mathrm{Im}(S_m^v). \tag{16}$$

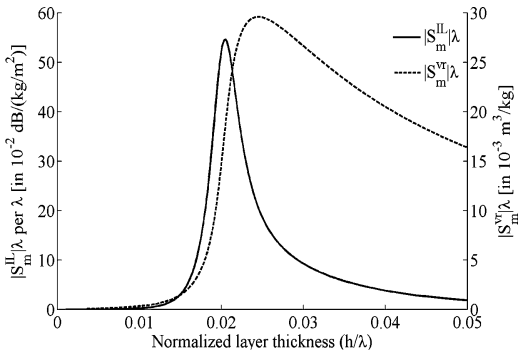

Fig. 2. Mass velocity and mass loss sensitivity of the fundamental Love mode in a polymer-coated device.

2.3. Numerical illustration for a polymer-coated Love wave sensor

By using Eqs. (15) and (16), normalized mass sensitivities are calculated for a Love wave device consisting of a polymeric layer, two IDTs with a period of $\lambda = 28\,\mu$m, and a piezoelectric substrate of ST-cut 90°X-propagate quartz. The material constants of the viscoelastic guiding layer are set as: $\rho = 1250\,\mathrm{kg/m^3}$, $\mu_0 = 0.2\,\mathrm{GPa}$, $\mu_1 = 65\,\mathrm{MPa}$, $\tau_1 = 0.9\,\mathrm{ns}$, and $\varepsilon_L = 3\varepsilon_0$, where ε_0 is the vacuum permittivity. The detectors of most sensors work at the fundamental mode, so only the sensitivities of the first Love mode are shown in Fig. 2. The solid curve represents the normalized mass loss sensitivity of the fundamental Love mode; the dashed curve represents the normalized mass velocity sensitivity. As the layer thickness increases, both the sensitivities exist peak values, which is similar to the previous studies [17,18]. As shown in the figure, the mass loss sensitivity will reduce rapidly when the layer is thicker than a certain value ($h/\lambda = 0.02$), which means that the insertion loss will not increase during gas adsorption. When h/λ exceeds 0.025, the mass velocity sensitivity will be decreased slowly.

3. Adsorption mechanism of gas on the SAW detector surface

3.1. BET adsorption equation and its improved form

When a gas contacts a solid, gas molecules will strike the solid surface continuously; most of the gas molecules will be bounced back immediately, a small portion of the gas molecules will be remained on the solid surface for some time before returning to the gas phase. The retention behavior is called adsorption. According to the difference in bonding forces, adsorptions can be divided into physical adsorptions and chemical adsorptions: the adsorption caused by the intermolecular forces is a physical adsorption; the adsorption generated by chemical bonding forces is a chemical adsorption. During the process of a chemical adsorption, some new molecules will be generated by the chemical reactions between the adsorbed gas molecules and the surface molecules of the solid. Since chemical bondages are much stronger than molecular diffusions, under normal temperature and pressure the new generated molecules will not automatically decompose into the original gas molecules and solid surface molecules when the gas leaves. Most of SAW gas sensors are required repeatable, so only the physical adsorption is applicable. For a physical adsorption, the gas adsorption amount is decided by the adsorption temperature, gas pressure (or gas concentration), and the surface area of the solid. Among all theoretical models for physical adsorptions, BET formula is the

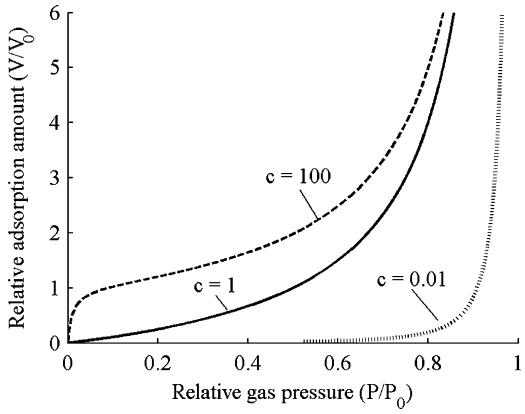

Fig. 3. BET adsorption isotherms of different adsorption constants.

most commonly used method, which was brought out by Brunauer, Emmett and Teller [27] in 1938:

$$\frac{V}{V_0} = \frac{cP/P_0}{(1-P/P_0)[1+(c-1)P/P_0]} \tag{17}$$

where V is the volume occupied by the adsorbed gas molecules; V_0 is the volume occupied by the gas molecules corresponding to a saturated monomolecular layer adsorption; P is the gas pressure; P_0 is the saturated vapor pressure at the adsorption temperature; c is an adsorption characteristic parameter.

At a certain temperature, the pressure of a gas is proportional to its concentration. According to the gas equation of state

$$P = \frac{\rho_C}{M}RT \tag{18}$$

where ρ_C is the mass volume concentration of the target gas; M is the mass of per mole gas molecules; R is the ideal gas constant; T is the adsorption temperature in the thermodynamic temperature scale.

Fig. 3 shows the BET adsorption isotherms calculated by using Eq. (17) with different adsorption constants. The numerical results show that the adsorption amount increases as the gas pressure increases. When the relative gas pressure tends to 1, the theoretical adsorption amount tends to infinity. The reason for this unreasonable result is the assumption that at $P = P_0$ an infinite number of layers are absorbed. The figure also displays that the isotherm with a greater adsorption constant is above on the isotherm with a smaller adsorption constant. The significance of this is the higher value of the adsorption constant, the lower detection limit of the target gas. Generally, the adsorption constant of a polar gas is less than 1, the adsorption constant of a non-polar gas is greater than 1.

For the two-parameter BET equation of Eq. (17), it is known that the best suitable interval of relative gas pressure is 0.05–0.35. To expand the suitable scope of BET adsorption equation, a variety of improvements were introduced. Wherein the Anderson adsorption equation, which was brought by Anderson [28] and Brunauer [29], is the most successful:

$$\frac{V}{V_0} = \frac{ckx}{(1-kx)[1+(c-1)kx]} \tag{19}$$

where k is an adjustable constant decided by the nature of the adsorption system, x represents the relative pressure P/P_0. By selecting the appropriate value of k, we can get the theoretical results consistent with the experimental data at x of 0.05–0.9.

3.2. Sensor response and surface area of the porous layer

Generally, SAW gas sensors measure the changes in the propagation velocity, phase, or oscillation frequency to determine the concentration of the target vapor. The sensor output is approximately proportional to the amount of absorbed gas: $\Delta v/\Delta v_0 = V/V_0$, because the adsorption amount is relative small in most cases. So we can know the sensor output of a given gas concentration (pressure) by using Eq. (17) or (19).

Assuming the absorbed gas molecules are small balls distributed on a solid surface closely, and the density of absorbed molecules is equal to the liquid density, the area occupied by a single molecule is [30]:

$$a_0 = 1.091\left(\frac{M}{N\rho_l}\right)^{2/3} \tag{20}$$

where M is the mass of per mole gas molecules, N is Avogadro's number, ρ_l is the liquid density of the target gas. The areal density of the monomolecular layer of the absorbed gas can be expressed as:

$$\sigma_0 = \frac{M/N}{a_0} = 0.9166\left(\frac{M\rho_l^2}{N}\right)^{1/3} \tag{21}$$

which will cause a change in the propagation velocity:

$$\Delta v_0 = v_r\sigma_0 S_m^{v_r} \tag{22}$$

and an increment in the insertion loss:

$$\Delta \mathrm{IL}_0 = \frac{d}{\lambda}\sigma_0 S_m^{\mathrm{IL}} \tag{23}$$

where d is the propagation distance of Love waves.

Generally, a polymer film is deposited on the surface of an SAW device by using a sol–gel method. After solvent evaporation, the remained layer is a porous medium, which has a surface area much larger than a dense medium. By fitting experimental data, we can get Δv_1, the experimental velocity change caused by a saturated monomolecular layer of absorbed gas. Thus we get the surface area of the porous polymer layer:

$$A_1 = \frac{\Delta v_1}{\Delta v_0}A_0 \tag{24}$$

where A_0 is the surface area of a solid layer.

4. Experiment verification

The experiments are performed on measuring the changes in propagation velocity and insertion loss of a Love wave device during vapor absorption with different relative humidity. The device consists of a substrate of quartz and an overlay of PVA, which is a known high molecular-weight hygroscopic polymer with the backbone chain consisting of $-[CH_2-CH]_n-$ and a C bonded OH group.

4.1. Experimental system

4.1.1. Love wave device

The Love wave device used in this work consists of an ST-cut and 90°X-propagate quartz substrate with two photolithographically defined Al (200 nm) interdigital transducers (IDTs) with an aperture of 2 mm. The IDTs are separated by a path length (transducer center separation) of 4 mm; each IDT consists of 72 periods of split-electrodes, with periodicity $\lambda = 28\,\mu$m (3.5 μm electrodes and spaces).

4.1.2. Polymer coating

The commercial PVA (average degree of polymerization 1750 ± 50, purity 97%) was obtained from Beijing Yili Fine Chemicals Co., Ltd. A solution was prepared by putting 30 g of PVA powder into 600 ml of deionized water contained in a glass baker. The solution was first heated to 60 °C and maintained for 40 min; then the solution was heated to 90 °C and maintained for 50 min, until the

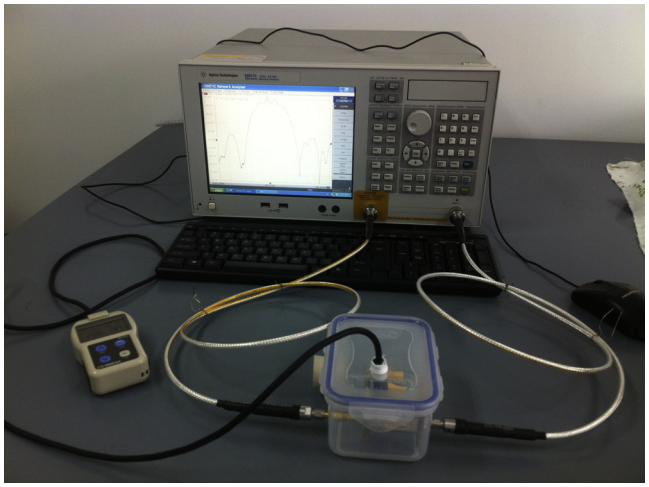

Fig. 4. Experiment system of the humidity sensor based on a PVA-coated Love wave device.

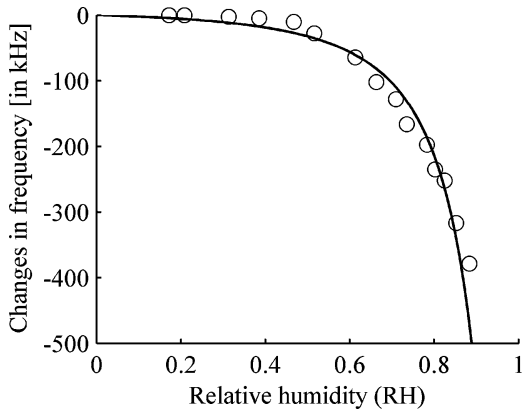

Fig. 5. Measured (circles) and calculated (solid line) frequency shifts vs relative humidity for the PVA-coated Love wave device.

PVA powder was completely dissolved. In the process of dissolution, the solution has been being shaken by a thermo magnetic stirrer. The prepared PVA solution was cooled in air for 3 h and the final volume of the remaining solution was about 480 ml. A thin layer of PVA solution was brushed on the surface of the IDT-fabricated quartz wafer; then the wafer was rotated at a speed of 4000 rpm for 20 s. After coating, the wafer is placed in air at 60 °C for 30 min to cure the PVA film. The film on the wire pad was removed by using a sharp scalped blade. The thickness of the prepared PVA layer is about 0.47 μm, which was measured by using an Alpha-step IQ surface profiler (KLA-Tencor, San Jose, CA).

4.1.3. Measurement equipment

The coated wafer was divided into several Love wave devices; then each device was mounted on a four-pin rectangular DIP header with electrical connections made by Al wires bonding. The header was soldered on a PCB; the input and output impedances of the Love device were matched to about 50 ohm by using LC circuits. As seen in Fig. 4, the PCB with the matched device was placed in a plastic container, which has four drilled holes. Passing through the two holes located in the opposite walls, two SMA connectors were applied to connect the Love wave device and an Agilent E5071C network analyzer. The probe of a standard hygrometer passes through the hole in the top wall and reaches the place near the device surface. The stand hygrometer is a digital thermo-hygrometer RH32B-2C (Omega Engineering, Inc., Stamford, CT), which is used as a reference to monitor the variations in relative humidity (RH) and temperature. The humidity inside the container was increased or decreased by adding wet sponge or silicone particles through the fourth hole in the side wall.

4.2. Experimental and numerical results

4.2.1. Changes in operation frequency

Fig. 5 shows the frequency shifts of the Love wave device as a function respect to the relative humidity in decimal form. RH is the ratio of moisture pressure in the air and saturated vapor pressure. The shifts in the device operation frequency represent the sensor output, which is proportional to the amount of absorbed gas: $\Delta f/\Delta f_1 = \Delta v/\Delta v_1 = V/V_1$.

The circles denote the frequency shifts measured through the humidity experiment, which is operated at the temperature of 22.9–23.2 °C. As RH = 0.17, the Love wave device works at a frequency of 178.15 MHz. The solid line is the theoretical curve calculated by using Eq. (19) with the parameters of $k = 0.96$, $\Delta f_1 = -200$ kHz and $c = 0.1$, which is less than 1 because water vapor is a polar molecular gas. When RH < 0.5, the frequency shift is relative small and is proportional to the relative humidity; when RH > 0.5, a rapid increase occurs in the frequency shift as the humidity increases.

4.2.2. Surface area of PVA film

PVA is relative soft polymer. In this work, the material constants of PVA are assumed as: the density $\rho = 1.25 \times 10^3$ kg/m^3, the complex shear modulus $\mu_0 = 0.2$ GPa, $\mu_1 = 65$ MPa, the relaxation time $\tau_1 = 0.9$ ns, the permittivity $\varepsilon = 3\varepsilon_0$. By using the method introduced in Section 2, we can get the magnitude of the normalized mass velocity sensitivity $\left|S_m^{v_r}\right| \lambda = 2.94 \times 10^{-3}$ m^2/kg, the magnitude of the normalized mass loss sensitivity $\left|S_m^{IL}\right| \lambda = 9.17 \times 10^{-2}$ dB m^2/kg at the PVA layer thickness of 0.47 μm ($h/\lambda = 0.0168$).

It is known that the water vapor has a mole mass of $M = 0.018$ kg/mol, a liquid density of $\rho_l = 1000$ kg/m^3; substituting these constants into Eq. (21), we can get the areal density of a single water molecules layer: $\sigma_0 = 2.845 \times 10^{-7}$ kg/m^2. The monolayer of water molecules causes a shift in the device operation frequency of

$$\Delta f_0 = -\frac{2.94 \times 10^{-3}}{28 \times 10^{-6}} \times 178.15 \times 10^3 \times 2.845 \times 10^{-7} = -5.32\,\text{kHz} \tag{25}$$

and an increment in the device insertion loss of

$$\Delta \text{IL}_0 = \frac{9.17 \times 10^{-2}}{28 \times 10^{-6}} \times \frac{4 \times 10^{-3}}{28 \times 10^{-6}} \times 2.845 \times 10^{-7} = 0.133\,\text{dB}. \tag{26}$$

By using Eq. (24), we can get the experimental surface area of the PVA layer: $A_1 = 37.6 A_0$, which will produce an experimental increment in device insertion loss of $\Delta \text{IL}_1 = 5.0$ dB.

4.2.3. Changes in insertion loss

The increment of the device insertion loss is displayed in Fig. 6 as a function respect to the relative humidity. The circles denote the experimental data; the solid line is calculated by using Eq. (19) with the parameters of $k = 0.96$, $\Delta \text{IL}_1 = 5.0$ dB and $c = 0.1$. As RH = 0.17, the origin insertion loss of the Love wave device is about 9.68 dB. The

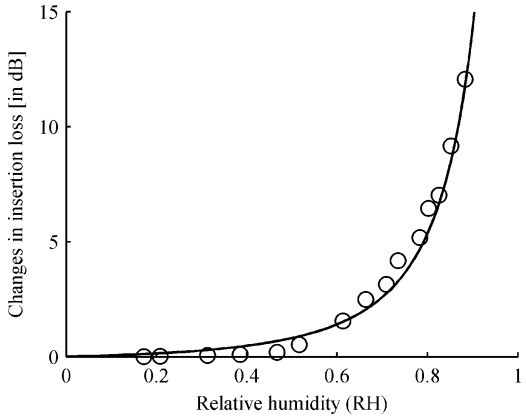

Fig. 6. Measured (circles) and calculated (solid line) insertion loss increments vs relative humidity for the PVA-coated Love wave device.

change trend of the insertion loss increment is similar to that of the operation frequency shift.

5. Conclusions

This work presents an investigation on the dynamics and response of a humidity sensor based on a polymer-coated Love wave device. For Love waves in a polymer-coated device, the viscosity of the polymeric layer will produce deviations in propagation velocity and mass sensitivity. The real part and imaginary part of the mass sensitivity correspond to the mass velocity sensitivity and mass loss sensitivity, respectively.

The adsorption of gas in the SAW detector surface is proved as a physical adsorption, which is described by the BET adsorption equation and its improved form, the Anderson equation. The absorption isotherm, which plots the relative adsorption amount as a function respect to the relative gas pressure, is characterized by the adsorption constant c. The c with a large value of tens or hundreds produces a large adsorption amount at a small gas pressure (concentration), which is helpful to get a small detecting limit; the c with a small value of less than 1 produces a good linearity in a wide range of gas pressure. The polymer deposited by using a sol–gel method is proved a porous material; the relative surface area of the polymer can be obtained by comparing the experimental frequency shift and the theoretical shift caused by the saturated monolayer of adsorbed gas molecules.

An experiment is performed on a humidity sensor based on a Love wave device consisting of two 28 μm-periodic IDTs, a 0.47 μm-thick PVA layer, and an ST-90°X quartz substrate. Figs. 5 and 6 display the changes in operation frequency and insertion loss of the Love wave device as functions respect RH respectively. The experimental parameters of the improved BET adsorption isotherm are $k = 0.96$, $c = 0.1$, $\Delta f_1 = -200$ kHz and $\Delta IL_1 = 5.0$ dB, which are frequency shift and insertion loss increment caused by a monolayer of water molecules. According to the theoretical method in Section 2, the monolayer produces a frequency shift of −5.32 kHz, and an increment in insertion loss of 0.133 dB. Using these parameters, we can get the surface area of the porous PVA layer of $37.6A_0$, where A_0 is the plane area of the substrate surface.

The method and discussion presented in this work are also applicable for other types of polymer-coated SAW gas sensors.

Acknowledgements

The authors are grateful to Mr. Yong Liang for fabricating the Love wave device, to Dr. Mengwei Liu, Dr. Junhong Li and Mr. Wei Ren for their help in experimental measurement. This work was partly financially supported by the National Natural Science Foundation of China (No. 11104314).

References

[1] S. Shiokawa, J. Kondoh, Surface acoustic wave sensors, Jpn. J. Appl. Phys. 43 (2004) 2799–2802.
[2] T.M.A. Gronewold, Surface acoustic wave sensors in the bioanalytical field: recent trends and challenges, Anal. Chim. Acta 603 (2007) 119–128.
[3] J.D.N. Cheeke, Z. Wang, Acoustic wave gas sensors, Sens. Actuators B 59 (1999) 146–153.
[4] R. Fachberger, A. Erlacher, Monitoring of the temperature inside a lining of a metallurgical vessel using a SAW temperature sensor, Procedia Chem. 1 (2009) 1239–1242.
[5] A. Binder, G. Bruckner, N. Schobernig, D. Schmitt, Wireless surface acoustic wave pressure and temperature sensor with unique identification based on $LiNbO_3$, IEEE Sens. J. 13 (2013) 1801–1805.
[6] B. Donohoe, D. Geraghty, G.E. O'Donnell, Wireless calibration of a surface acoustic wave resonator as a strain sensor, IEEE Sens. J. 11 (2011) 1026–1032.
[7] M. Kurosaws, Y. Fukula, M. Takasaki, A surface-acoustic-wave gyro sensor, Sens. Actuators A 66 (1998) 33–39.
[8] H. Wohltjen, R. Dessy, Surface wave probe for chemical analysis: I. Introduction and instrument description, II. Gas chromatography detector, Anal. Chem. 51 (9) (1979) 1458–1470.
[9] M. David, M. Arab, C. Martino, L. Delmas, F. Guinneton, J.R. Gavarri, Carbon nanotubes/ceria composite layers deposited on surface acoustic wave devices for gas detection at room temperature, Thin Solid Films 520 (2012) 4786–4791.
[10] C. Lee, G. Lee, Humidity sensors: a review, Sensor Lett. 3 (2005) 1–14.
[11] M. Penza, G. Cassano, Relative humidity sensing by PVA-coated dual resonator SAW oscillator, Sens. Actuators B 68 (2000) 300–306.
[12] R. Rimeikaa, D. Čiplys, V. Poderys, R. Rotomskis, M.S. Shur, Fast-response surface acoustic wave humidity sensor based on hematoporphyrin film, Sens. Actuators B 137 (2009) 592–596.
[13] A. Buvailo, Y. Xing, J. Hines, E. Borguet, Thin polymer film based rapid surface acoustic wave humidity sensors, Sens. Actuators B 156 (2011) 444–449.
[14] Y. Li, C. Deng, M. Yang, A novel surface acoustic wave-impedance humidity sensor based on the composite of polyaniline and poly(vinyl alcohol) with a capability of detecting low humidity, Sens. Actuators B 165 (2012) 7–12.
[15] S.J. Martin, G.C. Frye, S.D. Senturla, Dynamics and response of polymer-coated surface acoustic wave devices: effect of viscoelastic properties and film resonance, Anal. Chem. 66 (1994) 2201–2219.
[16] P. Kiełczyn'ski, Attenuation of Love waves in low-loss media, J. Appl. Phys. 82 (1997) 5932–5937.
[17] G. McHale, M.I. Newton, F. Martin, Theoretical mass, liquid, and polymer sensitivity of acoustic wave sensors with viscoelastic guiding layers, J. Appl. Phys. 93 (2003) 675–690.
[18] J. Liu, L. Wang, Y. Lu, S. He, Properties of Love waves in a piezoelectric layered structure with a viscoelastic guiding layer, Smart Mater. Struct. 22 (2013) 125034.
[19] J. Liu, A theoretical study on Love wave sensors in a structure with multiple viscoelastic layers on a piezoelectric substrate, Smart Mater. Struct. 23 (2014) 075015.
[20] Y. Wang, S. Zhang, F. Zhou, L. Fan, Y. Yang, C. Wang, Love wave hydrogen sensors based on ZnO nanorod film/36°YX-$LiTaO_3$ substrate structures operated at room temperature, Sens. Actuators B 158 (2011) 97–103.
[21] V. Chivukula, C. Kritzinger, F. Yavari, D. Čiplys, N. Koratkar, M.S. Shur, Detection of CO_2 absorption in graphene using surface acoustic waves, in: IEEE Ultrasonics Symp. Proc., San Diego, CA, USA, 11, 2010, pp. 257–260.
[22] L. Blanc, A. Tetelin, C. Boissière, G. Tortissier, C. Dejous, D. Rebière, Love wave characterization of the shear modulus variations of mesoporous sensitive films during vapor sorption, IEEE Sens. J. 12 (2012) 1442–1449.
[23] J. Liu, Y. Lu, Response mechanism for surface acoustic wave gas sensors based on surface-adsorption, Sensors 14 (2014) 6844–6853.
[24] J. Liu, S. He, Properties of Love waves in layered piezoelectric structures, Int. J. Solids Struct. 47 (2010) 169–174.
[25] J. Liu, S. He, Theoretical analysis on Love waves in a layered structure with a piezoelectric substrate and multiple elastic layers, J. Appl. Phys. 107 (2010) 073511.
[26] B. Jakoby, M.J. Vellekoop, Properties of Love waves: applications in sensors, Smart Mater. Struct. 6 (1997) 668–679.
[27] S. Brunauer, P.H. Emmett, E.J. Teller, Adsorption of gases in multimolecular layers, J. Am. Chem. Soc. 60 (1938) 309–319.
[28] R.B. Anderson, Modifications of the Brunauer, Emmett and Teller equation, J. Am. Chem. Soc. 68 (1946) 686–691.
[29] S. Brunauer, J. Skalny, E.E. Bodor, Adsorption on nonporous solids, J. Colloid Interface Sci. 30 (1969) 546–552.
[30] P.H. Emmetatn, D.S. Brunauer, The use of low temperature van der Waals adsorption isotherms in determining the surface area of iron synthetic ammonia catalysts, J. Am. Chem. Soc. 59 (1937) 1553–1564.

Biographies

Jiansheng Liu obtained his B.S. degree in Electrical Engineering from Tsinghua University (Beijing, China) in 2002, and his Ph.D. degree in Signal and Information Processing from Graduate University, Chinese Academy of Sciences (GUCAS, Beijing) in 2007. During 2007–2009, he was an assistant researcher at Institute of Acoustics, Chinese Academy of Sciences (IACAS, Beijing), where he has been an associated professor since 2010. His current research interests include sensors based on piezoelectric Love waves, response mechanism for SAW sensors, low loss SAW filters and SAW filter banks, parameters of SAW couple-of-mode (COM) model.

Lijun Wang obtained her B.S. degree in Communication Engineering from Shandong University (Weihai, China) in 2012. Now she is a graduate student in IACAS. Her research interests are experiments on Love wave-based sensors and SAW gas sensors.